



HAL
open science

Energy response and identification efficiency of CsI(Tl) crystals irradiated with energetic protons

C. Frosin, S. Barlini, G. Poggi, G. Casini, M. Bini, A.A. Stefanini, S. Valdré, D. Gruyer, M. Ciemala, A. Maj, et al.

► **To cite this version:**

C. Frosin, S. Barlini, G. Poggi, G. Casini, M. Bini, et al.. Energy response and identification efficiency of CsI(Tl) crystals irradiated with energetic protons. *Detection Systems and Techniques in Nuclear and Particle Physics*, Sep 2019, Messina, Italy. pp.012010, <10.1088/1742-6596/1561/1/012010>. <hal-02892961>

HAL Id: hal-02892961

<https://hal.science/hal-02892961v1>

Submitted on 29 May 2024

HAL is a multi-disciplinary open access archive for the deposit and dissemination of scientific research documents, whether they are published or not. The documents may come from teaching and research institutions in France or abroad, or from public or private research centers.

L'archive ouverte pluridisciplinaire **HAL**, est destinée au dépôt et à la diffusion de documents scientifiques de niveau recherche, publiés ou non, émanant des établissements d'enseignement et de recherche français ou étrangers, des laboratoires publics ou privés.



Distributed under a Creative Commons CC BY 4.0 - Attribution - International License

PAPER • OPEN ACCESS

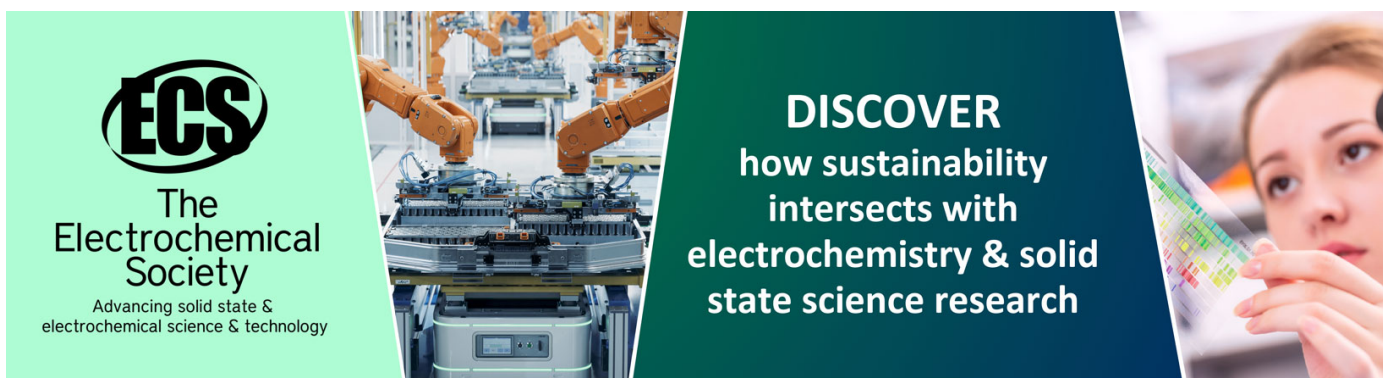
Energy response and identification efficiency of CsI(Tl) crystals irradiated with energetic protons

To cite this article: C Frosin *et al* 2020 *J. Phys.: Conf. Ser.* **1561** 012010

View the [article online](#) for updates and enhancements.

You may also like

- [Research on multi-probe energy response compensation for X/ dose rate meter](#)
M. Li, P. Gong, H. Zhang et al.
- [Neutron calibration facility with an Am-Be source for pulse shape discrimination measurement of CsI\(Tl\) crystals](#)
H.S. Lee, H. Bhang, J.H. Choi et al.
- [Experimental comparison of high-density scintillators for EMCCD-based gamma ray imaging](#)
Jan W T Heemskerck, Rob Kreuger, Marlies C Goorden et al.



ECS
The
Electrochemical
Society
Advancing solid state &
electrochemical science & technology

DISCOVER
how sustainability
intersects with
electrochemistry & solid
state science research

Energy response and identification efficiency of CsI(Tl) crystals irradiated with energetic protons

C Frosin^{1,2}, S Barlini^{1,2}, G Poggi^{1,2}, G Casini², M Bini^{1,2}, A A Stefanini^{1,2}, S Valdré², D Gruyer³, M Ciemała⁴, A Maj⁴, M Ziebliński⁴, B Sowicki⁴, K Mazurek⁴, N Cieplicka-Oryńczak⁴, M Matejska-Minda⁴, E Bonnet⁵, B Borderie⁶, R Bougault³, M Bruno^{7,8}, A Buccola^{1,2}, A Camaiani^{1,2}, A Chibhi⁹, M Cinausero¹¹, M Cicerchia^{10,11}, J Dueñas¹², D Fabris¹³, J Frankland⁹, F Gramegna¹¹, M Henri⁹, A Kordyasz¹⁴, N Le Neindre³, I Lombardo¹⁵, O Lopez³, G Mantovani^{10,11}, T Marchi¹¹, A Olmi², P Ottanelli^{1,2}, M Parlog^{3,16}, S Piantelli², G Pasquali^{1,2}, S Upadhyahya¹⁷, G Verde¹⁵ and E Vient³

¹ Dipartimento di Fisica, Universit di Firenze, I-50019 Sesto Fiorentino, Italy

² INFN Sezione di Firenze, I-50019 Sesto Fiorentino, Italy

³ LPC Caen, ENSICAEN, Universit de Caen, CNRS-IN2P3, F-14050 Caen cedex, France

⁴ Institute of Nuclear Physics, Polish Academy of Science, PL-31342 Krakow, Poland

⁵ Universit Nantes, EMN IN2P3 CNRS, SUBATECH, Nantes, France

⁶ IPNO, CNRS-IN2P3, Universit Paris-Sud 11, F-91406 Orsay cedex, France

⁷ Dipartimento di Fisica, Universit di Bologna, I-40126 Bologna, Italy

⁸ INFN Sezione di Bologna, I-40126 Bologna, Italy

⁹ GANIL, CEA/DSM-CNRS/IN2P3, F-14076 Caen cedex, France

¹⁰ Dipartimento di Fisica, Universit di Padova, I-35131 Padova, Italy

¹¹ INFN Laboratori Nazionali di Legnaro, I-35020 Legnaro, Italy

¹² Depto. de Ing. Eléctrica y Centro de Estudios Avanzatos en Física, Matemáticas y

Computación, Universidad de Huelva, S-21071 Huelva, Spain

¹³ INFN Sezione di Padova, I-35131 Padova, Italy

¹⁴ Heavy Ion Laboratory, University of Warsaw, PL-02093 Warsaw, Poland

¹⁵ INFN Sezione di Catania, I-95123 Catania, Italy

¹⁶ Horia Hulubei, IFIN-HH, RO-077125 Bucharest Magurele, Romania

¹⁷ Phys. Astr. and Appl. Comp. Sci., Jagiellonian University, PL-30348 Krakow, Poland

E-mail: frosin@infn.it

Abstract. Proton energy calibration and identification efficiency of few Thallium activated Cesium Iodide (CsI(Tl)) crystals of the FAZIA detection system, have been studied in the range 59-180 MeV by using the proton beam delivered by the cyclotron of the CCB (Cyclotron Center Bronowice) facility. We observe that the light output versus energy is linear in the lower investigated energy range while showing a deviation from linearity above 140 MeV. The effects of proton induced nuclear reactions and multiple scattering causing incomplete energy deposition (IED) events have been identified and estimated via Pulse Shape Analysis in CsI(Tl) crystals. The measured experimental efficiency for proton identification in the examined energy range is then compared with GEANT4 simulations. For a centered collimated irradiation on the crystal, and at the highest measured energy, the resulting experimental efficiency value is about 70%.



1. Introduction

Inorganic crystals such as CsI(Tl) are commonly used in nuclear physics, as part of many detector setups [1–3]. Typically, CsI(Tl) crystals are employed as the last layer of detector stacks in telescope configuration to detect and identify mainly charged reaction products from heavy ion collisions by means of either ΔE -E [4] or Pulse Shape Analysis techniques (PSA) [5]. One of the major drawbacks of the CsI(Tl) detectors, which can have a significant impact in spectroscopy, is related to the non-linear dependence of the light response with particle energy [6, 7]. Moreover, when used to detect high energy particles, the contribution from nuclear interactions or escaping particles, leading to a bad identification, is no longer negligible. In this context, we decided to perform a dedicated test using the FAZIA [1, 8] telescopes, made up by three stages of Si+Si+CsI(Tl). For this test, we used monochromatic proton beams delivered by the cyclotron of the CCB (Cyclotron Center Bronowice) facility. We present here the results relative to the energy calibration as a function of the proton energy, ranging from 59 to 180 MeV, near the punch-through energy (194 MeV) for 10 cm thick crystals. Moreover, we address the aspect of the incomplete energy deposition (IED) of protons in the crystals, which can be induced either by nuclear collisions of the impinging protons in the bulk or by the escape of these particles due to (multiple-) scattering. Extensive simulations with the GEANT4 toolkit [9] have been performed for a comparison with the experimental findings.

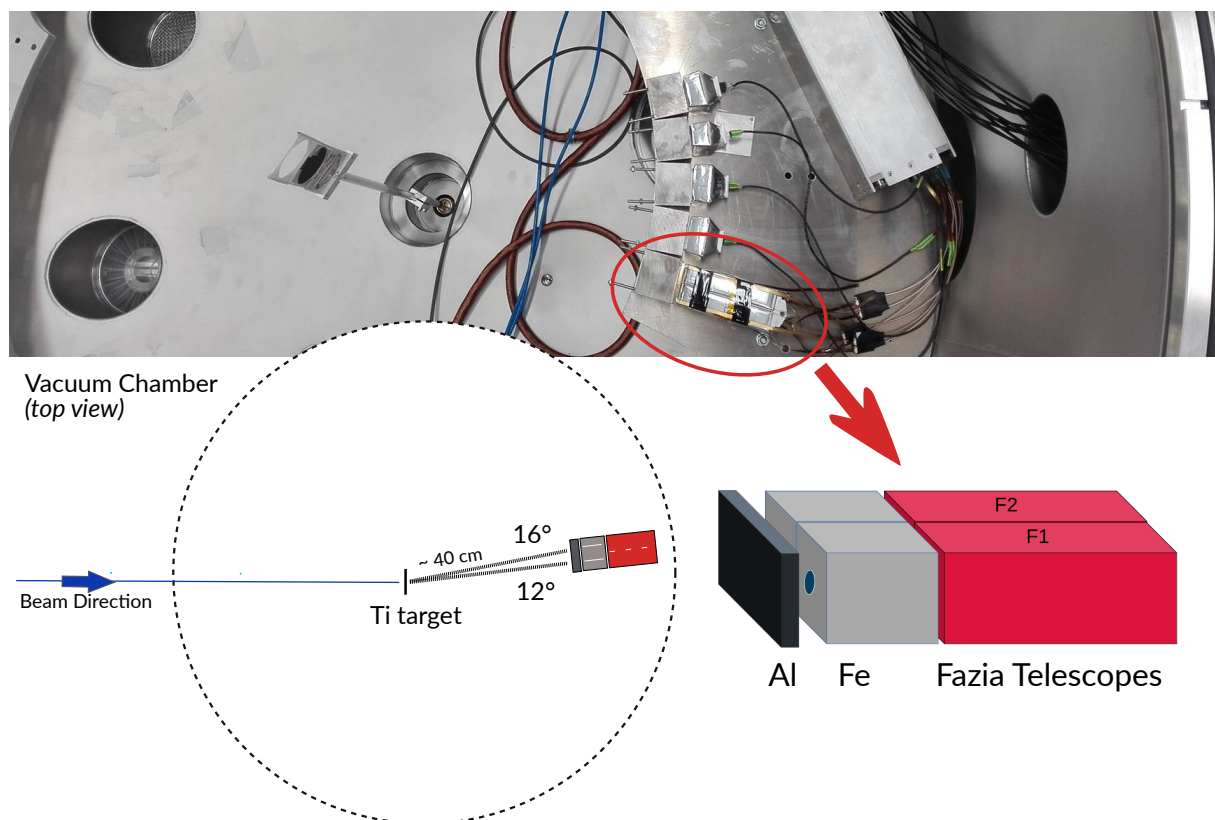


Figure 1: Picture and scheme of the layout of the experimental set-up (top view). The iron collimators (Fe) and the aluminum (Al) absorber are shown. They are placed in front of the two FAZIA telescopes during part of the experiment. The proton beam is scattered on a titanium target and reaches the FAZIA telescopes placed at 12° and 16° respectively on the equatorial plane of the scattering chamber. The other crystals shown in the picture are not for now considered in this paper.

2. Experimental setup

Two FAZIA telescopes (labeled as F1 and F2 after), each composed for this test by two equal Si stages (500 μm thick each) and a 10 cm thick CsI(Tl), were placed on the equatorial plane inside the scattering chamber of the experimental hall at CCB in Krakow (see Fig. 1). The two telescopes were 440 mm far from the target and were located at polar angles of 12° and 16° respectively, in order to optimize the counting rate. Proton beams, produced with variable energy between 70 MeV and 180 MeV, were elastically scattered by a ^{nat}Ti foil (4 cm diameter, 6.8 mg/cm^2 thickness). The telescopes were collimated with a passive iron block (Fe, 4 cm thick) with a 5 mm diameter hole so that only the central part of the active area was directly hit by protons. To reach the lower needed energies in some runs, we used Aluminum (Al) degraders placed in front of the telescopes (see Fig. 1). The crystals of FAZIA have a slight tapered shape, requested by the design distance from the target (100 cm), with front area being 20.4x20.4 mm^2 and the rear one being 21.7x21.7 mm^2 . The entrance face is protected by a reflecting aluminized Mylar foil (2 μm thick) while the lateral wrapping consists of high reflecting (98%) polymer foil (ESR Vikuiti 3M). The light collection readout is done by a custom photodiode (18x18 mm^2) which is coupled to the crystal with an optical cement. The fully digital electronics of a FAZIA block, described in details by [8], was used for the test with the triggers generated by the CsI(Tl) crystals. The waveforms of all silicon and CsI(Tl) detectors are acquired and continuously sampled and shaped via trapezoidal filters, whose maximum value provides the light output (LO hereafter) information expressed in terms of ADC units (ADU) of the sampler. The parameters of the filters were chosen according to the two types of detectors. We employed a rise-time of 2 μs and a flat top of 1 μs for the silicon detectors while for the CsI(Tl) signals, two trapezoidal shapers are active to separate the fast and slow components of the light output. The fast filter had a rise-time of 2 μs and a flat top of 0.5 μs . The slow filter instead had the same rise-time but a longer 10 μs flat top in order to be sensitive to the sum of the two light output components and to minimize the ballistic effect.

3. Results

3.1. Light output linearity

Figure 2 shows the proton energy spectra for F1 and F2 in the collimated geometry, at beam energies of 80 and 180 MeV. In the described experimental setup, protons elastically scattered by the target represent only a fraction of the detected events because other contributions arise from reactions in the target and from interaction with the iron collimator. To better understand the measured spectra, we decided to use the GEANT4 toolkit. With this code, we simulated the experimental conditions and we verified that a sizable contribution arises from protons scattered and partially degraded in a region next to the collimator hole (see Fig. 3). All of these effects, while contributing to form an extended low-energy tail in the measured proton spectra, yet do not prevent the detection of the sharp elastic peak needed for the energy calibration. The peak position can be extracted for every beam energy with a simple gaussian fit. Unfortunately, the background will play a major role in the efficiency calculation as we will see later.

The upper panel of Fig. 4 shows an example (for the F1 crystal) of the measured LO vs. energy for protons. The black points are the experimental results which are being compared with two fitting functions. The first is a linear correlation while the second one is a power law ($LO = a \cdot E^b$) with “a” and “b” free parameters as in Ref. [10]. The linear fit passing through the origin (red continuous line) well fits all the measured energies in the lower energy region, while one observes a systematically increasing deviation from a straight line for an energy higher than about 140 MeV. This is particularly evident in the bottom panel of the Fig. 4 where the residuals in ADU units (red triangles for the linear fit) are shown. This observation is in good agreement with results reported elsewhere [10]. The power law behaviour reproduces better the experimental data for the light output (blue dotted line in Fig. 4) produced in the CsI(Tl)

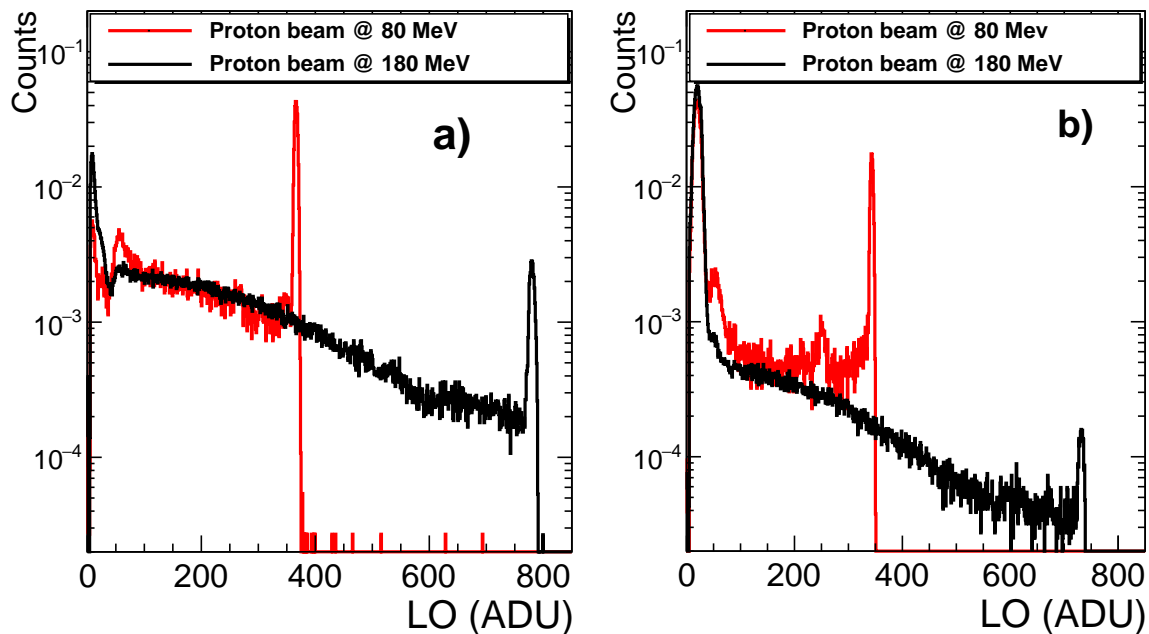


Figure 2: Proton Light Output spectra expressed in ADC units (ADU), measured with the two FAZIA CsI(Tl) detectors in the collimated configuration at two beam energies. Panel a) represents F1 at 12° and panel b) F2 at 16° . Histogram areas are normalized to 1. Figure taken from [11].

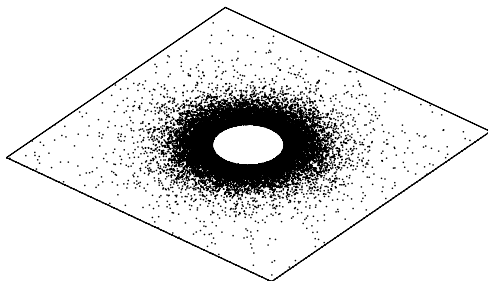


Figure 3: GEANT4 simulation showing the front face of the collimator hit by protons with a kinetic energy of 180 MeV. The points surrounding the hole represent the contribution of protons which are degraded and not fully stopped in the collimator, thus giving an energy tail in Fig. 2.

detector by light charged particles like protons. Moreover, the value of the exponent " b " is similar within the errors (0.9500.007 vs 0.9610.006 for F1 and F2) for the two FAZIA crystals, as expected for nominally identical crystals prepared according to the same procedure.

3.2. Proton identification efficiency

The impinging protons, before being fully stopped in the crystal can experience interactions which can be summarized as:

- Elastic (multiple-)scattering: change of the proton direction which consequently can cause the escape from the crystal
- Inelastic scattering and/or reactions: creation of both neutral (neutrons and γ) and/or secondary charged particles

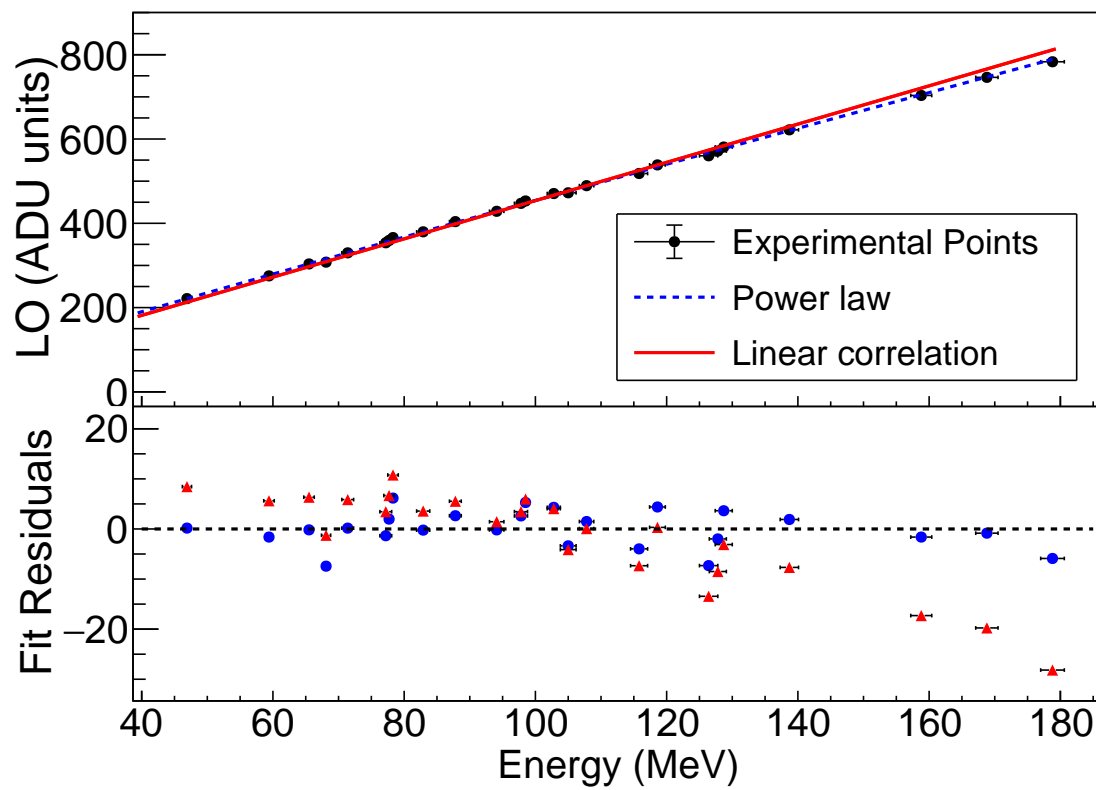


Figure 4: Upper panel: experimental correlation between the Light Output expressed in ADC units (ADU) and the proton energy (black points) for the F1 crystal. The red line represents a linear fit of the experimental points while the blue dotted line is a power law fit of the data. Bottom panel: residuals of the two fits (red triangles: linear fit, blue open dots: power law). Only the statistical errors are considered here (typically 0.5 ADU for y-axis) and the beam energy is known with a nominal accuracy of $\pm 1\%$ (for x-axis). For the lower energies, reached with the Al degraders, also the accuracy of the energy-loss calculations (typically 2-3%) has been taken into account. As a consequence, the uncertainty increases from 1% at 178 MeV to 1.5% at 47 MeV. Figure taken from [11].

These two effects are expected to contribute in different manners to the final signal amplitude in the CsI crystal. For example, when inelastic scattering or reactions are producing neutrons or γ , the energy deposited by the particle can be reduced because of the limited efficiency of the CsI(Tl) crystal for these types of particles/radiations. When secondary charged particles are produced the reduction of the light output is due to quenching effects which increase with charge and mass of the secondary particles. The effects due to nuclear reactions in CsI(Tl) have been already reported and extensively studied in the past (see Ref. [12,13]). On the other hand, the effects due to the elastic scattering processes were usually disregarded, because their importance strongly depends on the shape of the detector. Indeed, this phenomenon is enhanced when the transversal size is narrower than the longitudinal one. The consequence of both these effects is that part of the original energy is not released in the crystal, resulting in an IED (*Incomplete Energy Deposition*) event.

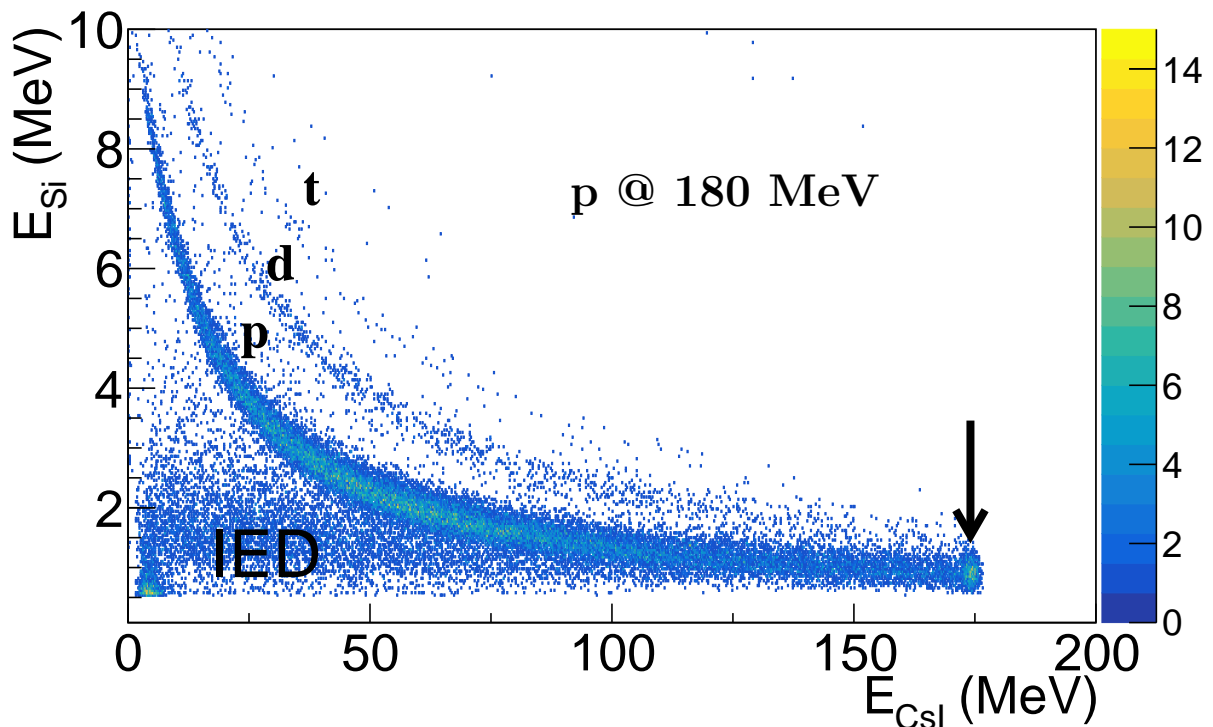


Figure 5: The sum of the energies deposited in the two silicons vs. LO (calibrated) correlation for the crystal F2 in the case of 180 MeV proton beam. The vertical arrow indicates the proton elastic peak, while letters indicate the ridges of the Hydrogen isotopes and the incomplete energy deposition events. Only events with an energy deposition in Silicon detectors higher than the noise level are reported.

In Fig. 5, a typical ΔE -E plot, obtained in our case for protons of 180 MeV is shown together with the associated locus of these IED events. One can clearly recognize the IED events as those with a correct energy deposition in the Si layer(s) but with a lower than expected energy deposition in the CsI(Tl) layer. These IED effects were further studied exploiting the PSA technique in the relevant detector as shown in Fig. 6. For the IED events a different combination of FLO (fast) and LO (slow) light output components is expected with respect to stopped particles. In fact, the stopped particles feature an energy deposition profile where the Bragg peak is fully contained inside the scintillator, resulting in a higher fast component. Therefore, as the fast component is larger for higher stopping power values, the fluorescence signal of an IED proton is expected to feature a reduced fast component with respect to a fully stopped proton depositing the same energy in the crystal. Events of this kind have been usually associated to gamma-rays because the corresponding produced electrons are indeed characterized by a smaller specific energy loss and consequently by a reduced fast component. However, from the calibrated x-axis of Figure 6 one can notice that these events extend almost up to the elastic peak energy. This actually excludes a sizable gamma-ray contribution which is rather expected in the same cut only at much smaller LO values (below 10 MeV). The only candidates for the higher energy region in the contour are therefore IED protons not having completely deposited their energy in the crystal.

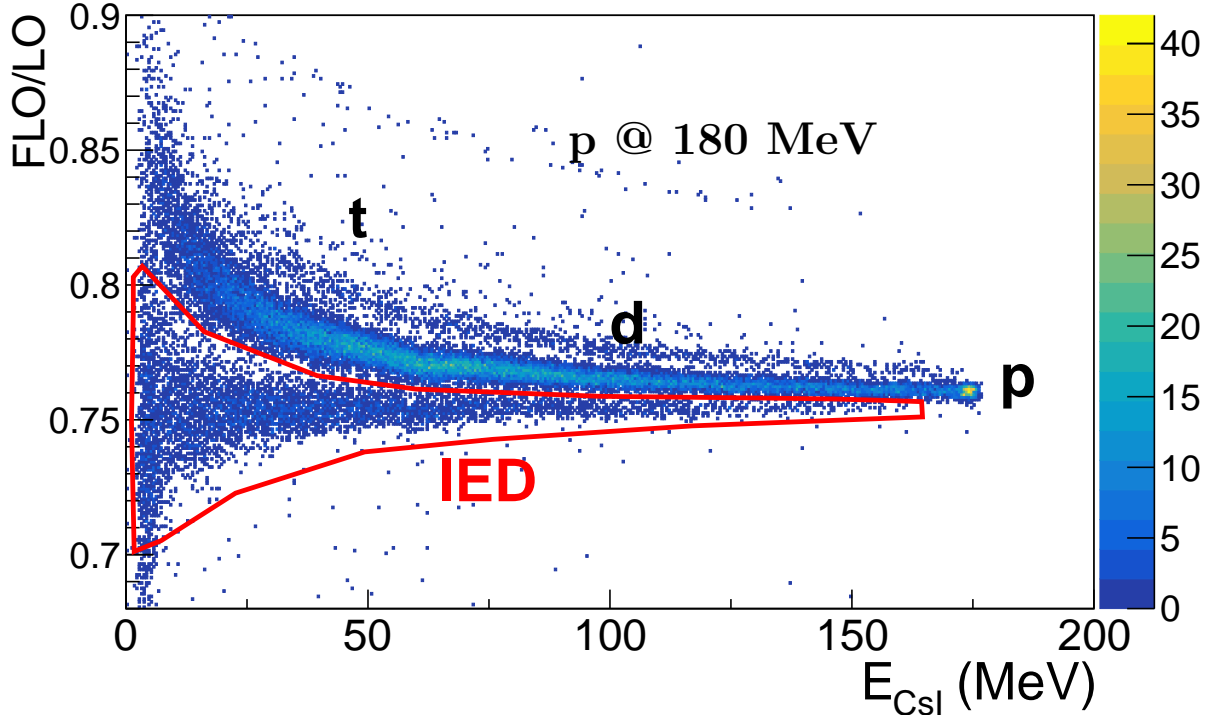


Figure 6: Matrix FLO/LO (or equivalently fast/slow) vs E_{CsI} for the crystal F2 measured at 180 MeV beam energy. The red contour indicates the position where most of the IED events from Figure 5, belong in the PSA correlation. The letters indicate the ridges of the Hydrogen isotopes.

For a simple case of monochromatic protons with an energy E_{el} , the efficiency for a proper detection of protons can be written as:

$$\eta_{el} = \frac{N_{CED}}{N_{in}} = \frac{N_{CED}}{N_{CED} + N_{IED}} \quad (1)$$

where N_{in} , N_{CED} and N_{IED} are the number of protons entering the crystal with a defined energy and the complete/incomplete energy deposition subsets. In a ΔE -E telescope the selection of the N_{in} protons entering the crystal with E_{CsI} can be performed by requiring the expected deposited energy ΔE_{Si} in the silicon detector(s), while the number N_{CED} is obtained by selecting from this ensemble the subset of protons populating the elastic peak. As we anticipated, in our case we observe a background due to the passive thick collimator; the energy distribution of protons impinging on the telescope extends to values lower than the elastic peak energy (see Fig. 5) and any selection of the deposited energy in silicons includes a non-vanishing fraction of these lower energy protons. This means that a clean selection results very difficult. First, we expect to have a systematic error in the efficiency evaluation. Secondly, we cannot assume the beam energy to be the reference point on the x-axis for the calculated efficiency due to the fact that to the IED events are contributing also non-elastic protons. In fact, experimentally we are rather dealing with the efficiency of a proton energy distribution strongly peaked at the beam energy but including a energy tail which shifts the mean value. For the fully description of the efficiency calculation procedure see Ref [11]. This is the reason why in Fig. 7, where the measured and GEANT4 calculated efficiencies are compared, the experimental points do not match the

energy of the simulated points. In principle, this lower energy proton contamination can be also

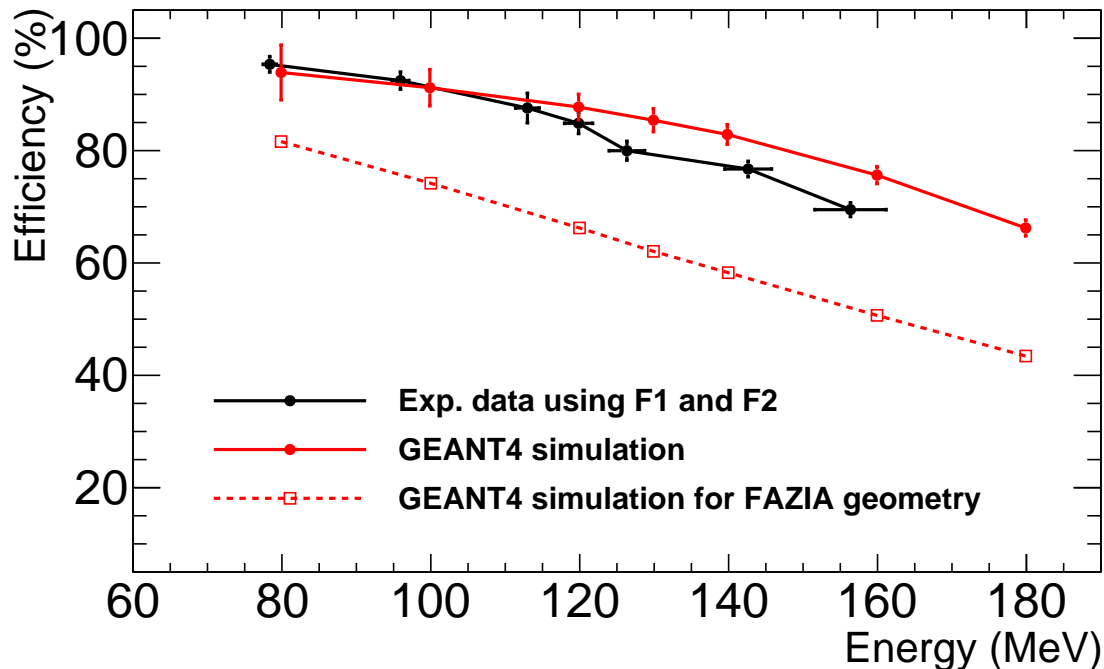


Figure 7: The experimental identification efficiencies (black symbols) compared with a GEANT4 simulation (red dots) in the collimated geometry. Open squares correspond to a GEANT4 simulation for the uncollimated geometry of FAZIA detectors. Connecting lines are drawn to guide the eye.

responsible for the slight disagreement between the measured and calculated efficiency, using the GEANT4 toolkit. This can be seen in Fig. 7, where the simulation is systematically lower than the experimental points. Nevertheless, if we trust the GEANT4 simulation, we can extend the calculation of the FAZIA CsI(Tl) efficiency for the crystal irradiated in the typical measurement condition corresponding to the telescopes mounted at 100 cm far from the target and without collimators. One can clearly notice from Fig. 7, how the elastic scattering plays an important role given the geometry of the crystal even at lower energies. For the simulation we used the *FTFP_BERT_EMZ* [14] physics list to mimic the interaction of protons in the CsI(Tl), including also the GEANT4 *option4* for optimized low-energy electromagnetic interaction. The proton beam is modeled as a monochromatic source located at 40 cm far from the iron collimator in the collimated geometry and at 100 cm for the open geometry.

4. Conclusions

Two CsI(Tl) crystals of the FAZIA array have been irradiated with proton beams of known energies, ranging from around 60 to 180 MeV. First, we verified that the expected linearity of the LO vs. energy correlation is satisfied in the lower energy region up to 110-120 MeV. Then, we found a deviation (less than 4%) increasing with the deposited energy, consistently with the results reported by [10]. The amount and similarity of these deviations suggest the necessity of deepening the study of their origin. Simulations with GEANT4 and lab tests with gamma-ray sources are in progress to check whether the non-linearity can be caused by the

light collection mechanism and particularly by the influence of the tapering of the crystals as already observed for similar detectors [15]. Secondly, we investigated the IED events, usually observed as a background in ΔE -E matrices. We pointed out that, instead of populating the stopped proton ridge in PSA correlation, they are positioned in the region pertaining, surely in its lower energy side, to gamma rays. This observation, to our knowledge has never been pointed out before and corrects some common misinterpretation of these events as merely due to neutral particles such as gamma or neutrons. The positioning of the IED events in this area has been explained as the result of a reduction of the fast scintillation component given by the lower density of energy loss of IED protons with respect to the fully stopped ones. Exploiting both the ΔE -E and PSA, we were able to determine the intrinsic identification efficiency of CsI(Tl) crystals for correctly detected protons, as a function of their impinging energy. The experimentally measured efficiency are reasonably supported by the GEANT4 calculations as the model is able to reproduce the trend, although an additional effort is required to understand the origin of the remaining systematic difference between experimental data and simulations. The reasons of this mismatch is still under study and a new experiment has been proposed for later this year at CCB using this time an active collimator for a cleaner experimental condition.

References

- [1] Bougault R *et al.* 2014 *Eur. J. Phys. A* **50** 47
- [2] Bruno M *et al.* 2013 *Eur. J. Phys. A* **49** 128
- [3] Wallace M S *et al.* 2007 *Nucl. Instrum. Methods A* **583** 302-12
- [4] Carboni S *et al.* 2012 *Nucl. Instrum. Methods A* **664** 251-63
- [5] Benrachi F *et al.* 1989 *Nucl. Instrum. Methods A* **281** 137-42
- [6] Prlog M *et al.* 2002 *Nucl. Instrum. Methods A* **482** 674-92
- [7] Prlog M *et al.* 2002 *Nucl. Instrum. Methods A* **482** 693-706
- [8] Valdre S *et al.* 2019 *Nucl. Instrum. Methods A* **930** 27-36
- [9] Agostinelli S *et al.* 2003 *Nucl. Instrum. Methods A* **506** 250-303
- [10] Dell'Aquila D *et al.* 2019 *Nucl. Instrum. Methods A* **929** 162-72
- [11] Frosin C *et al.* 2020 *Nucl. Instrum. Methods A* **951**, 163018
- [12] Siwek A *et al.* 2002 *NUKLEONIKA* **47** 141-45
- [13] Poggi G *et al.* 1993 *Nucl. Instrum. Methods A* **324** 177-90
- [14] Allison J *et al.* 2016 *Nucl. Instrum. Methods A* **835** 186-225
- [15] Diehl S *et al.* 2017 *Nucl. Instrum. Methods A* **857** 1-6